

CHARM PHYSICS: ANOTHER ROUTE TOWARDS NEW PHYSICS*

A.J. SCHWARTZ

Physics Department, University of Cincinnati, Cincinnati, Ohio 45221, USA

(Received April 24, 2018)

We summarize recent results for charm physics. These results span several categories: charm mixing, indirect (time-dependent) CP violation, direct (time-integrated) CP violation, T violation, semileptonic and leptonic decays, and decays of charm baryons.

DOI:10.5506/APhysPolB.49.1335

1. Introduction

Many new measurements of D -meson decays and charm baryon decays have been performed by the Belle, BaBar, LHCb, and BESIII experiments. Each experiment has unique advantages: Belle and BaBar produce boosted charmed hadrons in a low-background e^+e^- environment; LHCb produces very large event samples due the large $c\bar{c}$ production cross section in hadron collisions; and BESIII produces $D\bar{D}$ meson pairs in a quantum-correlated state at threshold with very little background. Here, we review recent results from all four experiments. The measurements can be grouped into six areas: measurements of charm mixing, indirect (time-dependent) CP violation, direct (time-integrated) CP violation, T violation, semileptonic and leptonic decays, and charm baryon decays. Our review highlights results that are sensitive to new physics and thus can constrain extensions to the Standard Model (SM).

2. Mixing and indirect CP violation

Measurements of mixing and CP violation require accurate flavor tagging and precise measurement of decay times. The former is usually achieved by reconstructing neutral D mesons originating from $D^{*+} \rightarrow D^0\pi^+$ and $D^{*-} \rightarrow$

* Presented at the Cracow Epiphany Conference on Advances in Heavy Flavour Physics, Kraków, Poland, January 9–12, 2018.

$\bar{D}^0\pi^-$ decays¹; the charge of the accompanying π^\pm tags the flavor of the D . The latter is achieved by measuring the displacement $\vec{\ell}$ between the D^{*+} and D^0 decay vertices and dividing by the D^0 momentum: $t = (\vec{\ell} \cdot \hat{p}_D)(M_{D^0}/p_D)$, where M_{D^0} is the D^0 mass [1]. The D^{*+} vertex position is taken to be the intersection of \vec{p}_D with the beam spot profile for e^+e^- experiments, and at the primary interaction vertex for $\bar{p}p$ and pp experiments.

CP violation (CPV) arises from interference between two or more decay amplitudes. When one of these amplitudes arises from mixing, then the resulting CPV is called *indirect*. Otherwise, when no mixing is involved, the CPV is called *direct*. Current measurements of charm mixing and *indirect* CPV determine mixing parameters x , y , or $x' = x \cos \delta + y \sin \delta$, $y' = y \cos \delta - x \sin \delta$, where δ is a strong phase; CPV parameters $|q/p|$ and $\text{Arg}(q/p) \equiv \phi$; and “mixed” observables $y_{\text{CP}} \approx y \cos \phi - (|q/p| - |p/q|)x \sin \phi/2$ and $A_\Gamma \approx (|q/p| - |p/q|)y \cos \phi/2 - x \sin \phi$. A value $|q/p| \neq 1$ gives rise to CPV in mixing, and a value $\phi \neq 0$ gives rise to CPV resulting from interference between a mixed amplitude and a direct decay amplitude. For further details of these quantities, see the review by the Heavy Flavor Averaging Group (HFLAV) [2]. Here, we present recent measurements of A_Γ , x'^2 , y' , and $|q/p|$ by LHCb [3–5], and results of a global fit for mixing and CPV parameters by HFLAV.

2.1. LHCb measurements

LHCb recently measured A_Γ using their full Run 1 dataset of 3.0 fb^{-1} [3]. This parameter is defined as $A_\Gamma \equiv (\hat{\tau}_{\bar{D}^0 \rightarrow f} - \hat{\tau}_{D^0 \rightarrow f})/(\hat{\tau}_{\bar{D}^0 \rightarrow f} + \hat{\tau}_{D^0 \rightarrow f})$, where $\hat{\tau}$ is the effective exponential lifetime of $D^0 \rightarrow f$ or $\bar{D}^0 \rightarrow f$ decays. This parameter can also be measured via the time-dependent CP asymmetry

$$A_{\text{CP}}(t) \equiv \frac{\Gamma(D^0(t) \rightarrow f) - \Gamma(\bar{D}^0(t) \rightarrow f)}{\Gamma(D^0(t) \rightarrow f) + \Gamma(\bar{D}^0(t) \rightarrow f)} \approx a_{\text{direct}}^f - A_\Gamma \left(\frac{t}{\tau_D} \right), \quad (1)$$

where a_{direct}^f represents the amount of direct CPV in the decay, and τ_D is the D^0 lifetime. This is the method used by LHCb. Here, one fits for D^0 and \bar{D}^0 yields in bins of decay time and calculates the difference in yields divided by the sum; the resulting background-free distribution is fit to Eq. (1). The method is much less sensitive to the decay time resolution function, which can be difficult to determine to high precision. The LHCb distribution is shown in Fig. 1. The fit results are $A_\Gamma(K^+K^-) = (-0.030 \pm 0.032 \pm 0.010)\%$ and $A_\Gamma(\pi^+\pi^-) = (0.046 \pm 0.058 \pm 0.012)\%$, where the first error is statistical and the second is systematic. Combining these gives $A_\Gamma = (-0.013 \pm 0.028 \pm 0.010)\%$, which is the most precise result for A_Γ to date.

¹ Throughout this paper, charge-conjugate modes are implicitly included unless stated otherwise.

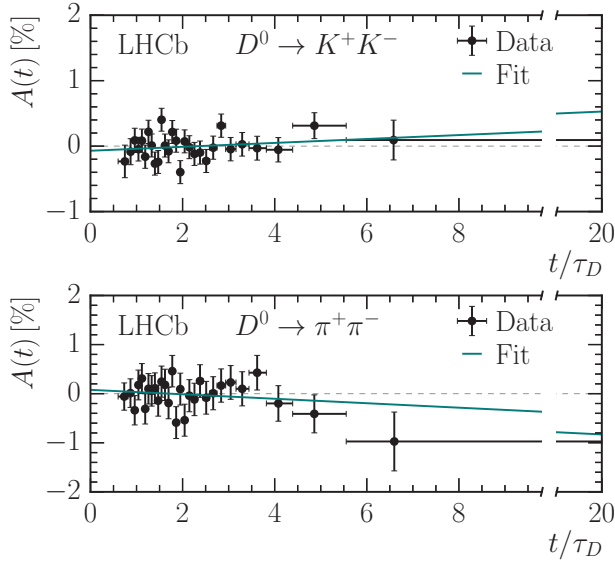


Fig. 1. $A_{CP}(t)$ for $D^0 \rightarrow K^+ K^-$ (top) and $D^0 \rightarrow \pi^+ \pi^-$ (bottom), from LHCb [3].

LHCb also recently measured mixing parameters x'^2 , y' , and the CPV parameter $|q/p|$ using “wrong-sign” $D^0 \rightarrow K^+ \pi^-$ decays and 3 fb^{-1} of data [4, 5]. Two separate analyses were performed, both using $D^{*+} \rightarrow D^0 \pi^+$ decays to tag the flavor of the D^0 . However, the second analysis required the D^* to originate from a $B \rightarrow D^{*+} \mu^- \nu$ decay, and thus the D^0 flavor was also tagged by the μ^+ . The signal yield of the first analysis is 720 000 events, while the yield for the “double-tagged” analysis is only 6680 events. However, upon combining the measurements, the latter adds $\sim 10\%$ in sensitivity due to very low background and increased acceptance at low D^0 decay times.

The ratio of wrong-sign $D^0 \rightarrow K^+ \pi^-$ decays to Cabibbo-favored “right-sign” decays $D^0 \rightarrow K^- \pi^+$, and the ratio for $\bar{D}^0 \rightarrow K^- \pi^+$ to $\bar{D}^0 \rightarrow K^+ \pi^-$ are, respectively [6],

$$R^+(t) = R_D + \left| \frac{q}{p} \right| \sqrt{R_D} (y' \cos \phi - x' \sin \phi) (\bar{\Gamma} t) + \left| \frac{q}{p} \right|^2 \frac{(x'^2 + y'^2)}{4} (\bar{\Gamma} t)^2 \quad (2)$$

$$R^-(t) = \bar{R}_D + \left| \frac{p}{q} \right| \sqrt{\bar{R}_D} (y' \cos \phi + x' \sin \phi) (\bar{\Gamma} t) + \left| \frac{p}{q} \right|^2 \frac{(x'^2 + y'^2)}{4} (\bar{\Gamma} t)^2, \quad (3)$$

where R_D is the ratio of amplitudes squared $|\mathcal{A}(D^0 \rightarrow K^+ \pi^-)|^2 / |\mathcal{A}(D^0 \rightarrow K^- \pi^+)|^2$, and $\bar{R}_D = |\mathcal{A}(\bar{D}^0 \rightarrow K^- \pi^+)|^2 / |\mathcal{A}(\bar{D}^0 \rightarrow K^+ \pi^-)|^2$. This measurement, like that for A_{Γ} , is also performed in bins of decay time. For each bin,

signal yields are obtained by fitting to variables M_D and $\Delta M = M_{D^*} - M_D$, and the ratios R^+ and R^- calculated. The resulting (background-free) decay time distributions are shown in Fig. 2. Simultaneously fitting these distributions to Eqs. (2) and (3) gives $x'^2 = (0.039 \pm 0.023 \pm 0.014) \times 10^{-3}$ and $y' = (0.528 \pm 0.045 \pm 0.027)\%$. From the single-tagged analysis alone, a loose constraint $|q/p| \in [0.82, 1.45]$ at 95% C.L. is obtained.

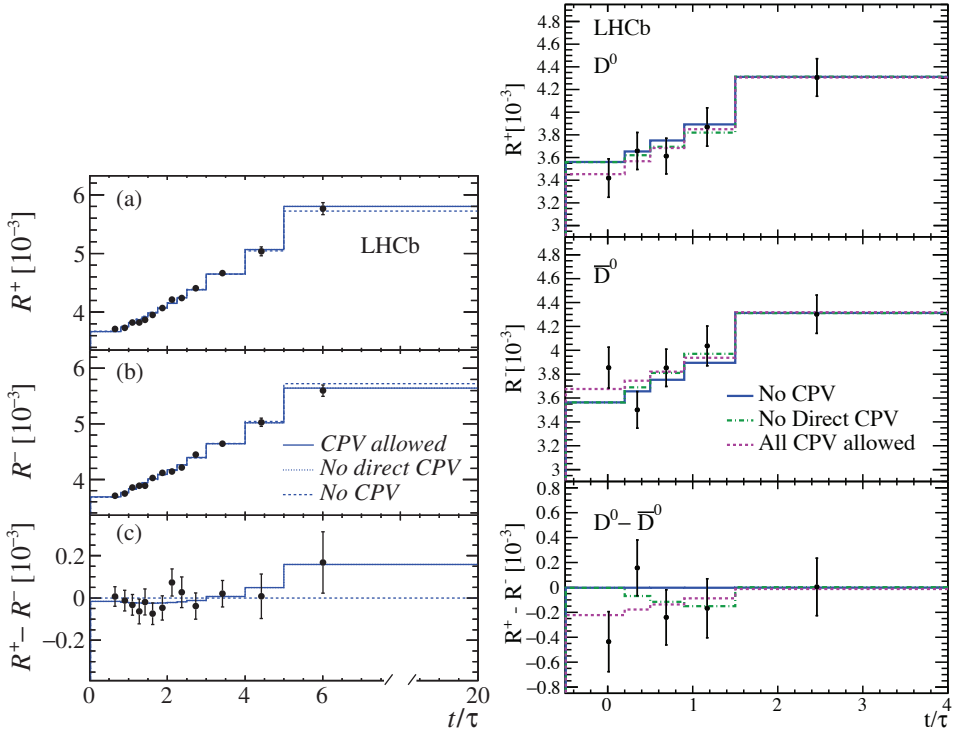


Fig. 2. Ratios $R^+(t)$ and $R^-(t)$ for singly tagged (left) and doubly tagged (right) $D^0 \rightarrow K^+ \pi^-$ decays, from LHCb [4, 5].

2.2. HFLAV global fit

HFLAV calculates world average values of A_Γ and also y_{CP} , and inputs all $D^0-\bar{D}^0$ mixing measurements into a global fit to determine world average values for 10 parameters: x , y , $|q/p|$, ϕ , R_D , direct CPV parameters A_D , A_K , and A_π , and strong phase differences δ and $\delta_{K\pi\pi}$. The fit uses 49 observables from measurements of $D^0 \rightarrow K^+ \ell^- \nu$, $D^0 \rightarrow K^+ K^-$, $D^0 \rightarrow \pi^+ \pi^-$, $D^0 \rightarrow K^+ \pi^-$, $D^0 \rightarrow K^+ \pi^- \pi^0$, $D^0 \rightarrow K_S^0 \pi^+ \pi^-$, $D^0 \rightarrow \pi^0 \pi^+ \pi^-$, $D^0 \rightarrow K_S^0 K^+ K^-$, and $D^0 \rightarrow K^+ \pi^- \pi^+ \pi^-$ decays, and double-tagged branching fractions measured at the $\psi(3770)$ resonance. Details are given in Ref. [2].

The results of the fit are listed in Table I. Several fits are performed: (a) assuming CP conservation by fixing $A_D = 0$, $A_K = 0$, $A_\pi = 0$, $\phi = 0$, and $|q/p| = 1$; (b) assuming no direct CPV in doubly Cabibbo-suppressed (DCS) decays ($A_D = 0$); (c) assuming no direct CPV in DCS decays and fitting for parameters $x_{12} = 2|M_{12}|/\Gamma$, $y_{12} = \Gamma_{12}/\Gamma$, and $\phi_{12} = \text{Arg}(M_{12}/\Gamma_{12})$, where M_{12} and Γ_{12} are the off-diagonal elements of the $D^0-\bar{D}^0$ mass and decay matrices, respectively; and (d) allowing full CPV (all parameters floated).

For fit (b), in addition to $A_D = 0$, HFLAV imposes the constraint [7, 8] $\tan \phi = (1 - |q/p|^2)/(1 + |q/p|^2) \times (x/y)$, which reduces four independent parameters to three². This constraint is imposed in two ways: first, floating x , y , and ϕ and from these deriving $|q/p|$; alternatively, floating x , y , and $|q/p|$ and from these deriving ϕ . The central values obtained from the two fits are identical, but the first fit yields (MINOS) errors for ϕ , while the second fit yields errors for $|q/p|$. For fit (c), HFLAV floats parameters x_{12} , y_{12} , and ϕ_{12} and from these calculates [8] x , y , $|q/p|$, and ϕ ; these are then compared to measured values. The 1σ - 5σ contours in the two-dimensional parameter spaces $(|q/p|, \phi)$ and (x_{12}, ϕ_{12}) are shown in Fig. 3. The HFLAV fit excludes the no-mixing point $x = y = 0$ at $> 11.5\sigma$, but the fit is consistent with CP conservation ($|q/p| = 1$, $\phi = 0$).

TABLE I

Results of the HFLAV global fit to 49 observables, from Ref. [2].

Parameter	No CPV	No direct CPV in DCS decays	All CPV allowed	CPV allowed [95% C.L.]
x [%]	$0.46^{+0.14}_{-0.15}$	$0.41^{+0.14}_{-0.15}$	0.32 ± 0.14	[0.04,0.62]
y [%]	0.62 ± 0.08	0.61 ± 0.07	$0.69^{+0.06}_{-0.07}$	[0.50,0.80]
$\delta_{K\pi}$ [°]	$8.0^{+9.7}_{-11.2}$	$4.8^{+10.4}_{-12.3}$	$15.2^{+7.6}_{-10.0}$	[-16.8,30.1]
R_D [%]	$0.348^{+0.004}_{-0.003}$	$0.347^{+0.004}_{-0.003}$	$0.349^{+0.004}_{-0.003}$	[0.342,0.356]
A_D [%]	—	—	-0.88 ± 0.99	[-2.8,1.0]
$ q/p $	—	0.999 ± 0.014	$0.89^{+0.08}_{-0.07}$	[0.77,1.12]
ϕ [°]	—	$0.05^{+0.54}_{-0.53}$	$-12.9^{+9.9}_{-8.7}$	[-30.2,10.6]
$\delta_{K\pi\pi}$ [°]	$20.4^{+23.3}_{-23.8}$	$22.6^{+24.1}_{-24.4}$	$31.7^{+23.5}_{-24.2}$	[-16.4,77.7]
A_π [%]	—	0.02 ± 0.13	0.01 ± 0.14	[-0.25,0.28]
A_K [%]	—	-0.11 ± 0.13	-0.11 ± 0.13	[-0.37,0.14]
x_{12} [%]	—	$0.41^{+0.14}_{-0.15}$	—	[0.10,0.67]
y_{12} [%]	—	0.61 ± 0.07	—	[0.47,0.75]
ϕ_{12} [°]	—	-0.17 ± 1.8	—	[-5.3,4.4]

² One can also use Eq. (15) of Ref. [9] to reduce four parameters to three.

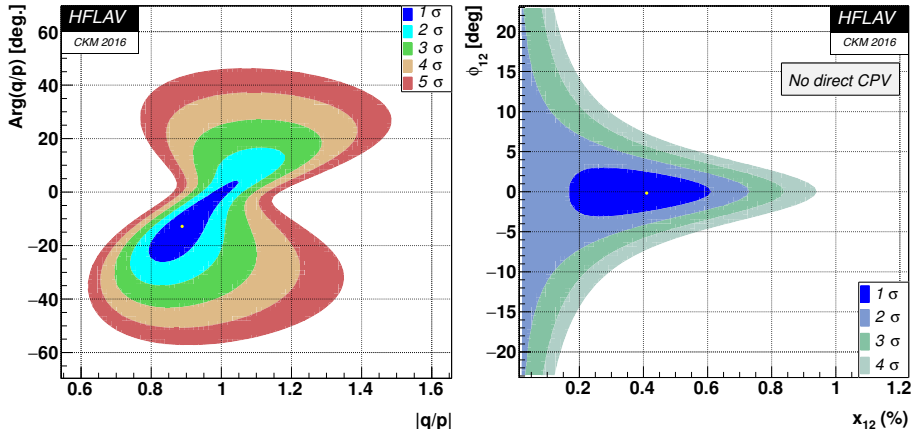


Fig. 3. (Colour on-line) Confidence contours resulting from the HFLAV global fit to 49 observables, from Ref. [2]. In the left plot, the blue contour shows consistency with CP conservation.

3. Direct CP violation

In addition to searches for indirect CPV in D decays, there have been many searches for direct CPV. Such searches consist of time-integrated measurements, *i.e.*, they do not require measuring decay times. However, flavor-tagging is important and, for high precision measurements, usually needs to be corrected for small systematic effects such as a possible charge asymmetry in the reconstruction of the low momentum π^\pm originating from $D^{*\pm} \rightarrow D\pi^\pm$ decays. The results to date are listed in Table II for D^0 decays, Table III for D^+ decays, and Table IV for D_s^+ decays. There are recent results from Belle ($D^0 \rightarrow K_S^0 K_S^0$ [10], $D^0 \rightarrow \rho^0/\phi/\bar{K}^{*0}\gamma$ [11], $D^+ \rightarrow \pi^+\pi^0$ [12]) and LHCb ($D^0 \rightarrow \pi^+\pi^-$ [13], $D^0 \rightarrow K^+K^-$ [13], $D^0 \rightarrow \pi^+\pi^-\pi^+\pi^-$ [14], $D_{(s)}^+ \rightarrow \eta'\pi^+$ [15]). In all cases, the results are consistent with no CPV. Several measurements have a precision of 0.2% or smaller.

4. T violation

Belle recently measured the T -violating parameter a_T for Cabibbo-favored $D^0 \rightarrow K_S^0 \pi^+ \pi^- \pi^0$ decays using their full dataset of 966 fb^{-1} [40]. The method used is similar to that used for earlier measurements of $D^0 \rightarrow K^+ K^- \pi^+ \pi^-$ decays (BaBar [41], LHCb [42]) and $D_{(s)}^+ \rightarrow K^+ K_S^0 \pi^+ \pi^-$ decays (BaBar [43]). This method is as follows. From the momenta of the daughter particles, one calculates the T -odd quantities

$$C_T \equiv \vec{p}_{K_S} \cdot (\vec{p}_{\pi^+} \times \vec{p}_{\pi^-}) \quad (4)$$

TABLE II

Time-integrated CP asymmetries for hadronic D^0 decays. The world averages are from HFLAV [27].

Decay	Channel	World avg. or most precise [%]	Most precise measurement
Cabibbo-favored	$D^0 \rightarrow K^- \pi^+$	0.3 ± 0.7	CLEO 2014 [16]
	$D^0 \rightarrow K_S^0 \pi^0$	-0.20 ± 0.17	Belle 2014 [17]
	$D^0 \rightarrow K^- \pi^+ \pi^0$	0.1 ± 0.5	CLEO 2014 [18]
	$D^0 \rightarrow K_S^0 \pi^+ \pi^-$	-0.08 ± 0.77	CDF 2012 [19]
	$D^0 \rightarrow K^- \pi^+ \pi^- \pi^+$	0.2 ± 0.5	CLEO 2014 [20]
	$D^0 \rightarrow \eta K_S^0$	0.54 ± 0.53	Belle 2011 [21]
	$D^0 \rightarrow \eta' K_S^0$	0.98 ± 0.68	Belle 2011 [21]
Singly Cabibbo-suppressed	$D^0 \rightarrow \pi^+ \pi^-$	0.00 ± 0.15	LHCb 2017 [13]
	$D^0 \rightarrow \pi^0 \pi^0$	-0.03 ± 0.64	Belle 2014 [17]
	$D^0 \rightarrow \pi^+ \pi^- \pi^0$	0.32 ± 0.42	{ LHCb 2015 [22] BaBar 2008 [23]
	$D^0 \rightarrow K_S^0 K_S^0$	-0.02 ± 1.54	Belle 2017 [10]
	$D^0 \rightarrow K^+ K^-$	-0.16 ± 0.12	LHCb 2017 [13]
	$D^0 \rightarrow K^+ K^- \pi^0$	-1.00 ± 1.69	BaBar 2008 [23]
	$D^0 \rightarrow K_S^0 K^\pm \pi^\pm$	—	LHCb 2016 [24]
	$D^0 \rightarrow \pi^+ \pi^- \pi^+ \pi^-$	—	LHCb 2017 [14]
	$D^0 \rightarrow K^+ K^- \pi^+ \pi^-$	—	LHCb 2013 [25]
Doubly Cabibbo-suppressed	$D^0 \rightarrow K^+ \pi^- \pi^0$	-0.14 ± 5.17	Belle 2005 [26]
	$D^0 \rightarrow K^+ \pi^- \pi^+ \pi^-$	-1.8 ± 4.4	Belle 2005 [26]
Radiative	$D^0 \rightarrow \rho^0 \gamma$	5.6 ± 15.2	Belle 2017 [11]
	$D^0 \rightarrow \phi \gamma$	-9.4 ± 6.6	Belle 2017 [11]
	$D^0 \rightarrow \bar{K}^{*0} \gamma$	-0.3 ± 2.0	Belle 2017 [11]

for $D^0 \rightarrow K_S^0 \pi^+ \pi^- \pi^0$ decays, and

$$\bar{C}_T \equiv \vec{p}_{K_S} \cdot (\vec{p}_{\pi^-} \times \vec{p}_{\pi^+}) \tag{5}$$

for $\bar{D}^0 \rightarrow K_S^0 \pi^- \pi^+ \pi^0$ decays. One integrates these quantities' distributions to construct the T -odd observables

$$A_T \equiv \frac{\Gamma(C_T > 0) - \Gamma(C_T < 0)}{\Gamma} \tag{6}$$

for D^0 decays, and

$$\bar{A}_T \equiv \frac{\bar{\Gamma}(-\bar{C}_T > 0) - \bar{\Gamma}(-\bar{C}_T < 0)}{\bar{\Gamma}} \tag{7}$$

TABLE III

Time-integrated CP asymmetries for hadronic D^+ decays. The world averages are from HFLAV [27].

Decay	Channel	World avg. or most precise [%]	Most precise measurement
Cabibbo-favored	$D^+ \rightarrow K_S^0 \pi^+$	-0.41 ± 0.09	Belle 2012 [28]
	$D^+ \rightarrow K_S^0 \pi^+ \pi^0$	-0.1 ± 0.7	CLEO 2014 [29]
	$D^+ \rightarrow K_S^0 \pi^+ \pi^+ \pi^-$	0.0 ± 1.2	CLEO 2014 [29]
	$D^+ \rightarrow K^- \pi^+ \pi^+$	-0.18 ± 0.16	D0 2014 [30]
	$D^+ \rightarrow K^- \pi^+ \pi^+ \pi^0$	-0.3 ± 0.7	CLEO 2014 [29]
Singly Cabibbo-suppressed	$D^+ \rightarrow \pi^+ \pi^0$	2.3 ± 1.3	Belle 2017 [12]
	$D^+ \rightarrow \pi^+ \pi^+ \pi^-$	—	LHCb 2014 [31]
	$D^+ \rightarrow K_S^0 K^+$	0.11 ± 0.17	LHCb 2014 [32]
	$D^+ \rightarrow K_S^0 K^+ \pi^+ \pi^-$	-4.2 ± 6.8	FOCUS 2005 [33]
	$D^+ \rightarrow K^+ K^- \pi^+$	0.32 ± 0.31	BaBar 2013 [34]
	$D^+ \rightarrow \eta \pi^+$	1.0 ± 1.0	Belle 2011 [35]
	$D^+ \rightarrow \eta' \pi^+$	-0.61 ± 0.90	LHCb 2017 [15]
Doubly Cabibbo-suppressed	$D^+ \rightarrow K^+ \pi^0$	-3.5 ± 10.7	CLEO 2010 [36]

for \bar{D}^0 decays. As illustrated in Fig. 4, these observables correspond to the difference between the K_S^0 momentum projecting above the (π^+, π^-) decay plane, and the momentum projecting below. Both A_T and \bar{A}_T may be nonzero due to either interference between strong phases in the decay amplitude, or T violation. A difference due to strong phases would be the same for A_T and \bar{A}_T , and thus the difference $a_T \equiv (A_T - \bar{A}_T)/2$ isolates the T -violating effect [44]. (This asymmetry is also CP-violating, so CPT conservation implies T violation.)

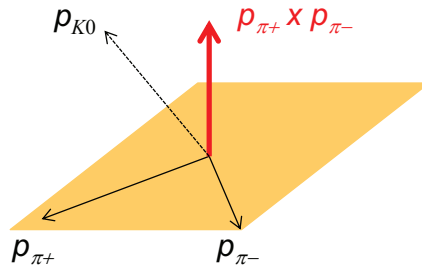


Fig. 4. Decay topology for $D^0 \rightarrow K_S^0 \pi^+ \pi^- \pi^0$.

TABLE IV

Time-integrated CP asymmetries for hadronic D_s^+ decays. The world averages are from HFLAV [27].

Decay	Channel	World avg. or most precise [%]	Most precise measurement
Cabibbo-favored	$D_s^+ \rightarrow K_S^0 K^+$	0.08 ± 0.26	BaBar 2013 [37]
	$D_s^+ \rightarrow K_S^0 K^+ \pi^0$	-1.6 ± 6.1	CLEO 2013 [38]
	$D_s^+ \rightarrow K_S^0 K_S^0 \pi^+$	3.1 ± 5.2	CLEO 2013 [38]
	$D_s^+ \rightarrow K^+ K^- \pi^+$	-0.5 ± 0.9	CLEO 2013 [38]
	$D_s^+ \rightarrow K^+ K^- \pi^+ \pi^0$	0.0 ± 3.0	CLEO 2013 [38]
	$D_s^+ \rightarrow K^- K_S^0 \pi^+ \pi^+$	4.1 ± 2.8	CLEO 2013 [38]
	$D_s^+ \rightarrow K_S^0 K^+ \pi^+ \pi^-$	-5.7 ± 5.4	CLEO 2013 [38]
	$D_s^+ \rightarrow \eta \pi^+$	1.1 ± 3.1	CLEO 2013 [38]
	$D_s^+ \rightarrow \eta \pi^+ \pi^0$	-0.5 ± 4.4	CLEO 2013 [38]
	$D_s^+ \rightarrow \eta' \pi^+$	-0.82 ± 0.50	LHCb 2017 [15]
	$D_s^+ \rightarrow \eta' \pi^+ \pi^0$	-0.4 ± 7.6	CLEO 2013 [38]
Singly Cabibbo-suppressed	$D_s^+ \rightarrow K_S^0 \pi^+$	0.38 ± 0.49	LHCb 2014 [39]
	$D_s^+ \rightarrow K^+ \pi^0$	-27 ± 24	CLEO 2010 [36]
	$D_s^+ \rightarrow K^+ \pi^+ \pi^-$	4.5 ± 4.8	CLEO 2013 [38]
	$D_s^+ \rightarrow \eta K^+$	9.3 ± 15.2	CLEO 2010 [36]
	$D_s^+ \rightarrow \eta' K^+$	6 ± 19	CLEO 2010 [36]
Annihilation	$D_s^+ \rightarrow \pi^+ \pi^- \pi^+$	-0.7 ± 3.1	CLEO 2013 [38]

The Belle measurement for $D^0 \rightarrow K_S^0 \pi^+ \pi^- \pi^0$ has good precision, as the signal yield is large and backgrounds are low. Belle fits for the signal yields of four independent subsamples: $\{D^0, C_T > 0\}$, $\{D^0, C_T < 0\}$, $\{\bar{D}^0, C_T > 0\}$, and $\{\bar{D}^0, C_T < 0\}$. The resulting yields give $a_T = (-0.028 \pm 0.138^{+0.023}_{-0.076})\%$, which is consistent with zero. As the four-body final state results mainly from two- and three-body intermediate states, Belle also divides the event sample into ranges of $M(\pi^+ \pi^- \pi^0)$, $M(\pi^\pm \pi^0)$, and $M(K_S^0 \pi^\pm)$ invariant masses to isolate $K_S^0 \omega$, $K_S^0 \eta$, $K^{*-} \rho^+$, $K^{*+} \rho^-$, $K^{*-} \pi^+ \pi^0$, $K^{*+} \pi^- \pi^0$, $K^{*0} \pi^+ \pi^-$, and $K_S^0 \rho^+ \pi^-$ intermediate states. For these subsamples, a_T is recalculated. The results are listed in Table V and are all consistent with zero, *i.e.*, no T violation is seen. Previous measurements of a_T for $D^0 \rightarrow K^+ K^- \pi^+ \pi^-$ [41, 42] and $D_{(s)}^+ \rightarrow K^+ K_S^0 \pi^+ \pi^-$ [43] also show no evidence for T violation.

TABLE V

Values of A_T and a_T for different regions of $D^0 \rightarrow K_S^0 \pi^+ \pi^- \pi^0$ phase space, from Belle [40]. $M_{ij[k]}$ indicates the invariant mass of mesons i and j [and k].

Resonance	Invariant mass range [GeV/ c^2]	A_T ($\times 10^{-2}$)	a_T ($\times 10^{-3}$)
$K_S^0 \omega$	$0.762 < M_{\pi^+ \pi^- \pi^0} < 0.802$	$3.6 \pm 0.5 \pm 0.5$	$-1.7 \pm 3.2 \pm 0.7$
$K_S^0 \eta$	$M_{\pi^+ \pi^- \pi^0} < 0.590$	$0.2 \pm 1.3 \pm 0.4$	$4.6 \pm 9.5 \pm 0.2$
$K^{*-} \rho^+$	$0.790 < M_{K_S^0 \pi^-} < 0.994$	$6.9 \pm 0.3^{+0.6}_{-0.5}$	$0.0 \pm 2.0^{+1.6}_{-1.4}$
	$0.610 < M_{\pi^+ \pi^0} < 0.960$	—	—
$K^{*+} \rho^-$	$0.790 < M_{K_S^0 \pi^+} < 0.994$	$22.0 \pm 0.6 \pm 0.6$	$1.2 \pm 4.4^{+0.3}_{-0.4}$
	$0.610 < M_{\pi^- \pi^0} < 0.960$	—	—
$K^{*-} \pi^+ \pi^0$	$0.790 < M_{K_S^0 \pi^-} < 0.994$	$25.5 \pm 0.7 \pm 0.5$	$-7.1 \pm 5.2^{+1.2}_{-1.3}$
$K^{*+} \pi^- \pi^0$	$0.790 < M_{K_S^0 \pi^+} < 0.994$	$24.5 \pm 1.0^{+0.7}_{-0.6}$	$-3.9 \pm 7.3^{+2.4}_{-1.2}$
$K^{*0} \pi^+ \pi^-$	$0.790 < M_{K_S^0 \pi^0} < 0.994$	$19.7 \pm 0.8^{+0.4}_{-0.5}$	$0.0 \pm 5.6^{+1.1}_{-0.9}$
$K_S^0 \rho^+ \pi^-$	$0.610 < M_{\pi^+ \pi^0} < 0.960$	$13.2 \pm 0.9 \pm 0.4$	$7.6 \pm 6.1^{+0.2}_{-0.0}$
Rest	—	$20.5 \pm 1.0^{+0.5}_{-0.6}$	$1.8 \pm 7.4^{+2.1}_{-5.3}$

5. Semileptonic and leptonic decays

Semileptonic and leptonic D decays are easier to understand theoretically than hadronic decays. Their decay rates are parameterized as

$$\frac{d\Gamma(D \rightarrow P \ell^+ \nu)}{dq^2} = \frac{G_F^2}{24\pi^3} |f^+(q^2)|^2 |V_{cs,cd}|^2 p^{*3} \quad (8)$$

and

$$\Gamma\left(D_{(s)}^+ \rightarrow \ell^+ \nu\right) = \frac{G_F^2}{8\pi} f_{D_{(s)}}^2 |V_{cs,cd}|^2 m_D m_\ell^2 \left(1 - \frac{m_\ell^2}{m_D^2}\right)^2, \quad (9)$$

where V_{cs} and V_{cd} are CKM matrix elements, p^* is the magnitude of the momentum of the final-state hadron in the D rest frame, $f^+(q^2)$ is a form factor evaluated at $q^2 = (P_D - P_P)^2 = (P_\ell + P_\nu)^2$, and $f_{D_{(s)}}$ is the $D_{(s)}^+$ decay constant. Thus, with knowledge of $f^+(q^2)$ or $f_{D_{(s)}}$ (*e.g.*, from lattice QCD calculations), measurements of semileptonic and leptonic decay rates determine $|V_{cd}|$ and $|V_{cs}|$. Alternatively, assuming values of $|V_{cd}|$ and $|V_{cs}|$ (*e.g.*, from CKM unitarity), the decay rates determine $f^+(q^2)$ and $f_{D_{(s)}}$. These values can be compared to theory predictions.

5.1. BESIII results

BESIII has recently presented new measurements of $D^+ \rightarrow \bar{K}^0 e^+ \nu$ and $D^+ \rightarrow \pi^0 e^+ \nu$ decays using hadronic tagging and 2.93 fb $^{-1}$ of data [45]. The

decay rates are measured in bins of q^2 , as shown in Fig. 5. The data points are fit to Eq. (8) using several theoretical models for $f^+(q^2)$; the floated parameters are the normalizations $f_+^K(q^2 = 0)|V_{cs}|$ and $f_+^\pi(q^2 = 0)|V_{cd}|$. Taking the form factor normalizations $f_+^K(0)$ and $f_+^\pi(0)$ from lattice QCD calculations [46, 47], one obtains $|V_{cs}| = 0.944 \pm 0.005 \pm 0.015 \pm 0.024$ and $|V_{cd}| = 0.210 \pm 0.004 \pm 0.001 \pm 0.009$, where the third error is due to theoretical uncertainty in the lattice calculations. These values are consistent with CKM unitarity (see below).

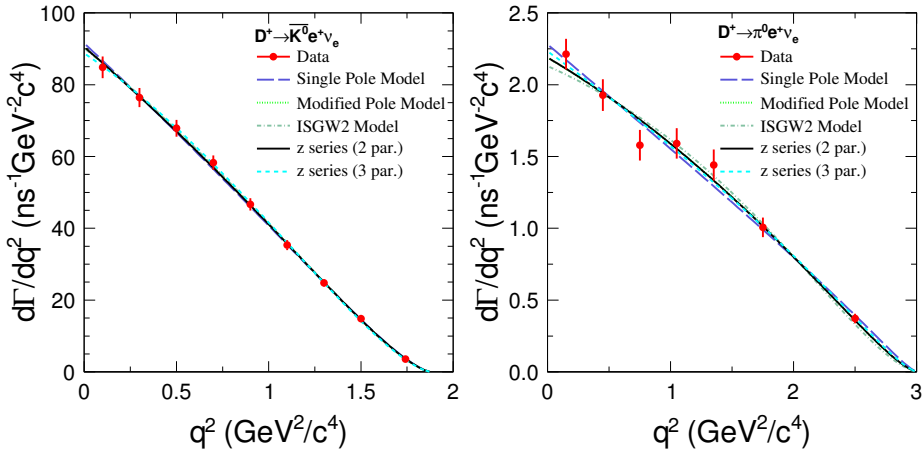


Fig. 5. BESIII results [45] for $D^+ \rightarrow \bar{K}^0 e^+ \nu$ decays (left) and $D^+ \rightarrow \pi^0 e^+ \nu$ decays (right). The theoretical predictions with floated normalizations $f_K^+(0)|V_{cs}|$ and $f_\pi^+(0)|V_{cd}|$ are superimposed.

Several other semileptonic decays have also been measured by BESIII, although no form factor calculations for these exist: $D^+ \rightarrow \phi(\mu^+, e^+) \nu$ [48], $D^+ \rightarrow \eta^{(\prime)} \mu^+ \nu$ [48], $D^+ \rightarrow \eta^{(\prime)} e^+ \nu$ [49], $D^+ \rightarrow \bar{K}^0 \mu^+ \nu$ [50], and the radiative leptonic decay $D^+ \rightarrow \gamma e^+ \nu$ [51]. BESIII results for purely leptonic decays $D_s^+ \rightarrow \mu^+ \nu$ and $D_s^+ \rightarrow \tau^+ \nu$ are given in Ref. [52].

5.2. HFLAV world averages

HFLAV has calculated world averages for the product $f_D|V_{cd}|$ measured using $D^+ \rightarrow \mu^+ \nu$ decays, and for the product $f_{D_s}|V_{cs}|$ measured using $D_s^+ \rightarrow e^+ \nu / \mu^+ \nu / \tau^+ \nu$ decays [2]. In the former case, inserting the lattice result $f_D = 212.15 \pm 1.45$ MeV [53] gives $|V_{cd}| = 0.2164 \pm 0.0050 \pm 0.0015$, which is consistent with the unitarity constraint $|V_{cd}| = 0.22492 \pm 0.00050$ [54]. Averaging this result with the corresponding value from semileptonic $D \rightarrow \pi \ell \nu$ decays gives a world average of 0.216 ± 0.005 , as shown in Fig. 6. This

value is also consistent with unitarity. Alternatively, inserting the unitarity value for $|V_{cd}|$ gives $f_D = 203.7 \pm 4.9$ MeV, which is 1.7σ lower than the lattice QCD prediction.

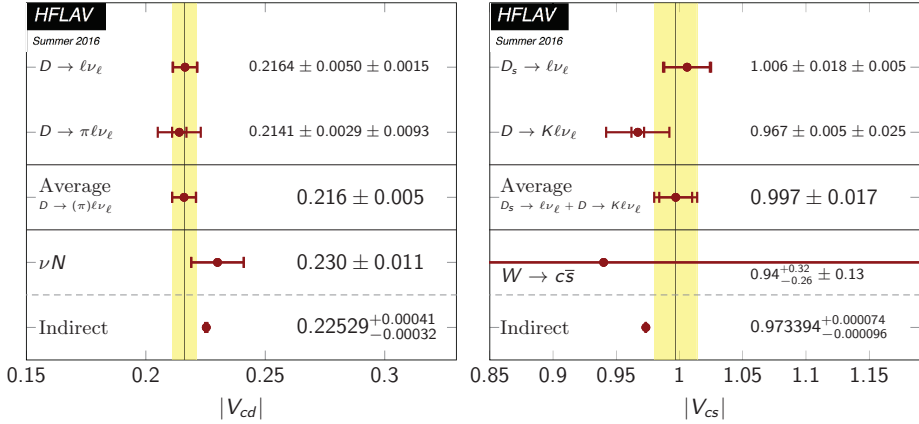


Fig. 6. HFLAV world average values for $|V_{cd}|$ (left) and $|V_{cs}|$ (right), from Ref. [2].

For $D_s^+ \rightarrow \ell^+ \nu$ decays, using the lattice result $f_{D_s} = 248.83 \pm 1.27$ MeV [53] gives $|V_{cs}| = 1.006 \pm 0.018 \pm 0.005$, which is consistent with the unitarity constraint $|V_{cs}| = 0.97351 \pm 0.00013$ [54]. Averaging this result with the corresponding value from $D \rightarrow K \ell \nu$ decays gives a world average of 0.997 ± 0.017 (see Fig. 6), which is also consistent with unitarity. Alternatively, inserting the unitarity value for $|V_{cs}|$ gives $f_{D_s} = 257.1 \pm 4.6$ MeV, which is 1.7σ higher than the lattice QCD prediction.

6. Charm baryons

There has recently been a profusion of new measurements of charm baryon decays. Belle, BESIII, and LHCb dominate these measurements, and their most recent results are listed in Table VI.

One result from Belle is that of a search for a “hidden-strangeness” pentaquark (P_s^+) with quark content $s\bar{s}uud$ [59]. This state would be analogous to the “hidden charm” pentaquark $P_c^+ = c\bar{c}uud$ observed by LHCb [77]. For this analysis, Belle reconstructed $\Lambda_c^+ \rightarrow \phi p \pi^0$ decays and fitted for the signal yield in bins of $M(\phi p)$ invariant mass. Plotting these yields gives a background-free $M(\phi p)$ distribution; a peaking structure would indicate an intermediate $P_s^+ \rightarrow \phi p$ decay. The resulting distribution is shown in Fig. 7. There is an excess of events (78 ± 28) at $M_{\phi p} = 2.025 \pm 0.005$ GeV/ c^2 , but the significance is only 2.7σ . The future Belle II experiment [78], with much higher statistics, should be able to clarify whether this excess is the first hint of a P_s^+ state.

TABLE VI

Recent results for charm baryon decays, from Belle (upper section), LHCb (middle section), and BESIII (bottom section).

Result	Data [fb^{-1}]	Experiment
$\Lambda_c^+ \rightarrow \Sigma \pi \pi$	711	Belle 2018 [55]
$\Xi_c(2930) \rightarrow \Lambda_c^+ K^-$	711	Belle 2018 [56]
Excited Ω_c	980	Belle 2018 [57]
Ω_c^0 hadronic decays	980	Belle 2018 [58]
$\Lambda_c^+ \rightarrow \phi p \pi^-, K^- \pi^+ \pi^0$	915	Belle 2017 [59]
$e^+e^- \rightarrow \Lambda_c^+ \Sigma_c^0, \Xi_c^0, \Omega_c^0$	800	Belle 2017 [60]
Excited Ξ_c^0, Ξ_c^+	980	Belle 2016 [61]
$\Xi_c(3055) \rightarrow \Lambda D$	980	Belle 2016 [62]
$\Lambda_c^+ \rightarrow p K^+ \pi^-$	980	Belle 2016 [63]
$\Lambda_c^+ \rightarrow p \mu^+ \mu^-$	3.0	LHCb 2017 [64]
$\Lambda_c^+ \rightarrow p K^+ K^-, p \pi^+ \pi^-$ CPV	3.0	LHCb 2017 [65]
$\Lambda_c^+ \rightarrow p K^+ K^-, p \pi^+ \pi^-, p \pi^- K^+$	1.0	LHCb 2018 [66]
Ξ_{cc}^{++}	1.7	LHCb 2017 [67]
Excited $\Omega_c^0 \rightarrow \Xi_c^+ K^-$	3.3	LHCb 2017 [68]
$\Lambda_c^+ \rightarrow \Xi^0 K^+, \Xi^0(1530) K^+$	0.567	BESIII 2018 [69]
$\Lambda_c^+ \rightarrow \Sigma^- \pi^+ \pi^+ \pi^0$	0.567	BESIII 2017 [70]
$\Lambda_c^+ \rightarrow p \eta, p \pi^0$	0.567	BESIII 2017 [71]
$\Lambda_c^+ \rightarrow \Lambda \mu^+ \nu$	0.567	BESIII 2017 [72]
$\Lambda_c^+ \rightarrow n K_S^0 \pi^+$	0.567	BESIII 2017 [73]
$\Lambda_c^+ \rightarrow p K^+ K^-, p \pi^+ \pi^-$	0.567	BESIII 2016 [74]
$\Lambda_c^+ \rightarrow h h h$	0.567	BESIII 2016 [75]
$\Lambda_c^+ \rightarrow \Lambda e^+ \nu$	0.567	BESIII 2015 [76]

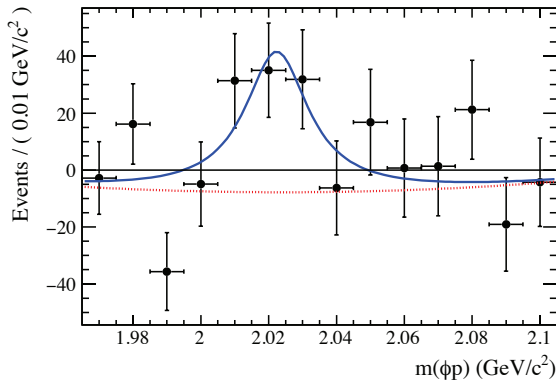


Fig. 7. Background-free $M(\phi p)$ invariant mass distribution for $D^0 \rightarrow \phi p \pi^0$ decays, from Belle [59].

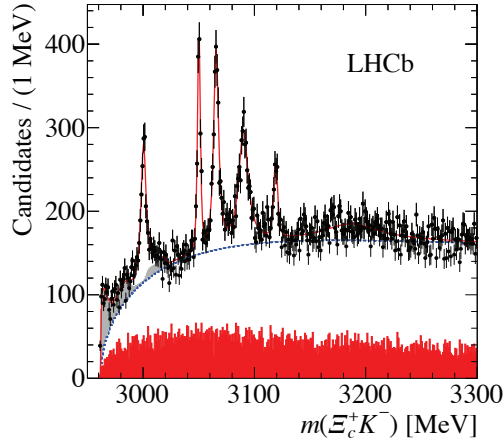


Fig. 8. $M(\Xi_c^+ K^-)$ invariant mass distribution, from LHCb [68].

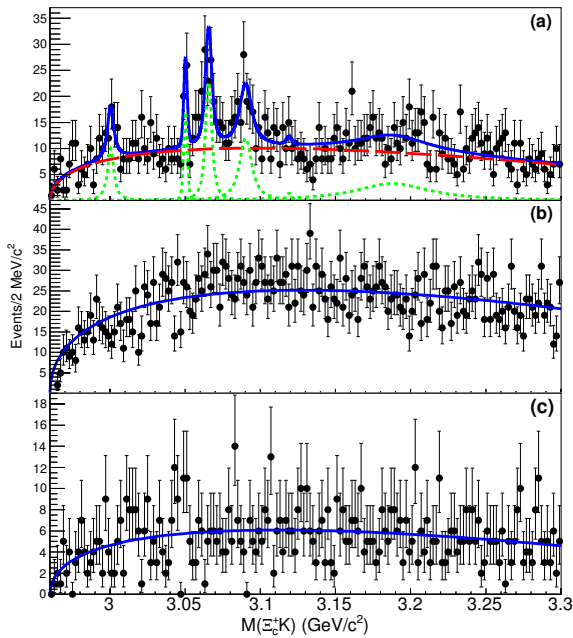


Fig. 9. (Colour on-line) Belle measurement [57] of excited Ω_c^* states. Top: $M(\Xi_c^+ K^-)$ invariant mass distribution. Middle: wrong-sign $M(\Xi_c^+ K^+)$ mass distribution, which contains only background. Bottom: $M(\Xi_c^+ K^-)$ mass distribution in which the " Ξ_c^+ " is taken from the $M(pK^- \pi^+)$ sideband. The solid (blue) curves show the overall fit projections.

Another interesting result comes from both LHCb [68] and Belle [58] and concerns excited Ω_c^* states, which have a valence quark content of css . LHCb observed five new excited states by reconstructing $\Xi_c^+ \rightarrow pK^-\pi^+$ decays, pairing the Ξ_c^+ with well-identified K^- tracks, and calculating the $M(\Xi_c^+K^-)$ invariant mass. The resulting distribution is shown in Fig. 8. Five narrow peaks are observed, clearly indicating $\Omega_c^* \rightarrow \Xi_c^+K^-$ decays. This result was recently confirmed by Belle (see Fig. 9), although the Belle statistics are significantly lower and only sufficient to identify four of the five Ω_c^* states.

7. Summary

Recent world averages for $D^0-\bar{D}^0$ mixing and indirect CPV parameters as calculated by HFLAV are summarized in Table I. Results from searches for direct CPV are summarized in Tables II, III, and IV. The most recent world averages for $|V_{cd}|$ and $|V_{cs}|$ as calculated from measurements of semileptonic and leptonic decays are plotted in Fig. 6; the resulting values are consistent with CKM unitarity. Finally, the most recent results for charm baryon decays are listed in Table VI. Although no statistically significant signal of new physics is seen, the precision of these results will be significantly improved with the analysis of LHCb Run 2 data and the large e^+e^- dataset to be collected by Belle II. Many new charm baryon measurements are expected, well beyond those listed in Table VI.

We thank the workshop organizers for hosting a productive meeting with excellent hospitality. The author also thanks Andrea Contu for reviewing this manuscript.

REFERENCES

- [1] C. Patrignani *et al.* [Particle Data Group], *Chin. Phys. C* **40**, 100001 (2016) and 2017 update.
- [2] Y. Amhis *et al.* [Heavy Flavor Averaging Group], *Eur. Phys. J. C* **77**, 895 (2017) [arXiv:1612.07233 [hep-ex]].
- [3] R. Aaij *et al.* [LHCb Collaboration], *Phys. Rev. Lett.* **118**, 261803 (2017).
- [4] R. Aaij *et al.* [LHCb Collaboration], *Phys. Rev. D* **97**, 031101 (2018).
- [5] R. Aaij *et al.* [LHCb Collaboration], *Phys. Rev. D* **95**, 052004 (2017).
- [6] S. Bergmann *et al.*, *Phys. Lett. B* **486**, 418 (2000).
- [7] M. Ciuchini *et al.*, *Phys. Lett. B* **655**, 162 (2007).
- [8] A. Kagan, M.D. Sokoloff, *Phys. Rev. D* **80**, 076008 (2009).
- [9] Y. Grossman, Y. Nir, G. Perez, *Phys. Rev. Lett.* **103**, 071602 (2009).

- [10] N. Dash *et al.* [Belle Collaboration], *Phys. Rev. Lett.* **119**, 171801 (2017).
- [11] T. Nanut *et al.* [Belle Collaboration], *Phys. Rev. Lett.* **118**, 051801 (2017).
- [12] V. Babu *et al.* [Belle Collaboration], *Phys. Rev. D* **97**, 011101 (2018).
- [13] R. Aaij *et al.* [LHCb Collaboration], *Phys. Lett. B* **767**, 177 (2017).
- [14] R. Aaij *et al.* [LHCb Collaboration], *Phys. Lett. B* **769**, 345 (2017).
- [15] R. Aaij *et al.* [LHCb Collaboration], *Phys. Lett. B* **771**, 21 (2017).
- [16] G. Bonvicini *et al.* [CLEO Collaboration], *Phys. Rev. D* **89**, 072002 (2014).
- [17] N.K. Nisar *et al.* [Belle Collaboration], *Phys. Rev. Lett.* **112**, 211601 (2014).
- [18] G. Bonvicini *et al.* [CLEO Collaboration], *Phys. Rev. D* **89**, 072002 (2014).
- [19] T. Aaltonen *et al.* [CDF Collaboration], *Phys. Rev. D* **86**, 032007 (2012).
- [20] G. Bonvicini *et al.* [CLEO Collaboration], *Phys. Rev. D* **89**, 072002 (2014).
- [21] B.R. Ko *et al.* [Belle Collaboration], *Phys. Rev. Lett.* **106**, 211801 (2011).
- [22] R. Aaij *et al.* [LHCb Collaboration], *Phys. Lett. B* **740**, 158 (2015).
- [23] B. Aubert *et al.* [BaBar Collaboration], *Phys. Rev. D* **78**, 051102 (2008).
- [24] R. Aaij *et al.* [LHCb Collaboration], *Phys. Rev. D* **93**, 052018 (2016).
- [25] R. Aaij *et al.* [LHCb Collaboration], *Phys. Lett. B* **726**, 623 (2013).
- [26] X.C. Tian *et al.* [Belle Collaboration], *Phys. Rev. Lett.* **95**, 231801 (2005).
- [27] Heavy Flavor Averaging Group,
<http://www.slac.stanford.edu/xorg/hflav/charm/index.html>
- [28] B.R. Ko *et al.* [Belle Collaboration], *Phys. Rev. Lett.* **109**, 021601 (2012).
- [29] G. Bonvicini *et al.* [CLEO Collaboration], *Phys. Rev. D* **89**, 072002 (2014).
- [30] V.M. Abazov *et al.* [DØ Collaboration], *Phys. Rev. D* **90**, 111102 (2014).
- [31] R. Aaij *et al.* [LHCb Collaboration], *Phys. Lett. B* **728**, 585 (2014).
- [32] R. Aaij *et al.* [LHCb Collaboration], *J. High Energy Phys.* **1410**, 025 (2014).
- [33] J.M. Link *et al.* [FOCUS Collaboration], *Phys. Lett. B* **622**, 239 (2005).
- [34] J.P. Lees *et al.* [BaBar Collaboration], *Phys. Rev. D* **87**, 052010 (2013).
- [35] E. Won *et al.* [Belle Collaboration], *Phys. Rev. Lett.* **107**, 221801 (2011).
- [36] H. Mendez *et al.* [CLEO Collaboration], *Phys. Rev. D* **81**, 052013 (2010).
- [37] J.P. Lees *et al.* [BaBar Collaboration], *Phys. Rev. D* **87**, 052012 (2013).
- [38] P.U.E. Onyisi *et al.* [CLEO Collaboration], *Phys. Rev. D* **88**, 032009 (2013).
- [39] R. Aaij *et al.* [LHCb Collaboration], *J. High Energy Phys.* **1410**, 025 (2014).
- [40] K. Prasanth *et al.* [Belle Collaboration], *Phys. Rev. D* **95**, 091101 (2017).
- [41] P. del Amo Sanchez *et al.* [BaBar Collaboration], *Phys. Rev. D* **81**, 111103 (2010).
- [42] R. Aaij *et al.* [LHCb Collaboration], *J. High Energy Phys.* **1410**, 005 (2014).
- [43] J.P. Lees *et al.* [BaBar Collaboration], *Phys. Rev. D* **84**, 031103 (2011).
- [44] W. Bensalem, D. London, *Phys. Rev. D* **64**, 116003 (2001).
- [45] M. Ablikim *et al.* [BESIII Collaboration], *Phys. Rev. D* **96**, 012002 (2017).
- [46] H. Na *et al.* [HPQCD Collaboration], *Phys. Rev. D* **82**, 114506 (2010).

- [47] H. Na *et al.* [HPQCD Collaboration], *Phys. Rev. D* **84**, 114505 (2011).
- [48] M. Ablikim *et al.* [BESIII Collaboration], *Phys. Rev. D* **97**, 012006 (2018).
- [49] M. Ablikim *et al.* [BESIII Collaboration], *Phys. Rev. D* **94**, 112003 (2016).
- [50] M. Ablikim *et al.* [BESIII Collaboration], *Eur. Phys. J. C* **76**, 369 (2016).
- [51] M. Ablikim *et al.* [BESIII Collaboration], *Phys. Rev. D* **95**, 071102 (2017).
- [52] M. Ablikim *et al.* [BESIII Collaboration], *Phys. Rev. D* **94**, 072004 (2016).
- [53] S. Aoki *et al.* [FLAG Working Group], *Eur. Phys. J. C* **77**, 112 (2017).
- [54] A. Ceccucci, Z. Ligeti, Y. Sakai, “CKM Quark-Mixing Matrix” in: C. Patrignani *et al.* [Particle Data Group], *Chin. Phys. C* **40**, 100001 (2016) and 2017 update.
- [55] M. Berger *et al.* [Belle Collaboration], [arXiv:1802.03421](https://arxiv.org/abs/1802.03421) [hep-ex].
- [56] Y.B. Li *et al.* [Belle Collaboration], *Eur. Phys. J. C* **78**, 252 (2018).
- [57] J. Yelton *et al.* [Belle Collaboration], *Phys. Rev. D* **97**, 032001 (2018).
- [58] J. Yelton *et al.* [Belle Collaboration], *Phys. Rev. D* **97**, 051102 (2018).
- [59] B. Pal *et al.* [Belle Collaboration], *Phys. Rev. D* **96**, 051102 (2017).
- [60] M. Niiyama *et al.* [Belle Collaboration], *Phys. Rev. D* **97**, 072005 (2018).
- [61] J. Yelton *et al.* [Belle Collaboration], *Phys. Rev. D* **94**, 052011 (2016).
- [62] Y. Kato *et al.* [Belle Collaboration], *Phys. Rev. D* **94**, 032002 (2016).
- [63] S.B. Yang *et al.* [Belle Collaboration], *Phys. Rev. Lett.* **117**, 011801 (2016).
- [64] R. Aaij *et al.* [LHCb Collaboration], *Phys. Rev. D* **97**, 091101 (2018).
- [65] R. Aaij *et al.* [LHCb Collaboration], *J. High Energy Phys.* **1803**, 182 (2018).
- [66] R. Aaij *et al.* [LHCb Collaboration], *J. High Energy Phys.* **1803**, 043 (2018).
- [67] R. Aaij *et al.* [LHCb Collaboration], *Phys. Rev. Lett.* **119**, 112001 (2017).
- [68] R. Aaij *et al.* [LHCb Collaboration], *Phys. Rev. Lett.* **118**, 182001 (2017).
- [69] M. Ablikim *et al.* [BESIII Collaboration], [arXiv:1803.04299](https://arxiv.org/abs/1803.04299) [hep-ex].
- [70] M. Ablikim *et al.* [BESIII Collaboration], *Phys. Lett. B* **772**, 388 (2017).
- [71] M. Ablikim *et al.* [BESIII Collaboration], *Phys. Rev. D* **95**, 111102 (2017).
- [72] M. Ablikim *et al.* [BESIII Collaboration], *Phys. Lett. B* **767**, 42 (2017).
- [73] M. Ablikim *et al.* [BESIII Collaboration], *Phys. Rev. Lett.* **118**, 112001 (2017).
- [74] M. Ablikim *et al.* [BESIII Collaboration], *Phys. Rev. Lett.* **117**, 232002 (2016).
- [75] M. Ablikim *et al.* [BESIII Collaboration], *Phys. Rev. Lett.* **116**, 052001 (2016).
- [76] M. Ablikim *et al.* [BESIII Collaboration], *Phys. Rev. Lett.* **115**, 221805 (2015).
- [77] R. Aaij *et al.* [LHCb Collaboration], *Phys. Rev. Lett.* **115**, 072001 (2015).
- [78] <https://www.belle2.org/>